

MECHANICAL TECHNOLOGY INCORPORATED
968 Albany-Shaker Road
Latham, New York

MTI-65TR25

**ANALYSIS AND DESIGN DATA
FOR THE AXIAL-EXCURSION TRANSDUCER
OF SQUEEZE-FILM BEARINGS**

by

**T. Chiang
C.H.T. Pan**

June 2, 1965

ANALYSIS AND DESIGN DATA FOR THE AXIAL-
EXCURSION TRANSDUCER OF SQUEEZE-FILM BEARINGS

by

T. Chiang
C.H.T. Pan

T. Chiang *C.H.T. Pan*
Author(s)

J. W. Freund
Approved by

Approved by

Prepared for

National Aeronautics and Space Administration,
George C. Marshall Space Flight Center

Prepared under

Contract NAS 8-11678

MECHANICAL TECHNOLOGY INCORPORATED
LATHAM, N.Y.

TABLE OF CONTENTS

	<u>Page</u>
ACKNOWLEDGEMENT -----	iv
ABSTRACT -----	v
INTRODUCTION -----	1
GENERAL ANALYSIS -----	3
SIMPLIFIED ANALYSIS -----	11
DESIGN DATA, PROCEDURES AND ILLUSTRATIVE EXAMPLES -----	14
CONCLUSIONS -----	20
REFERENCES -----	21
APPENDIX -----	22
FIGURES	
NOMENCLATURE	

ACKNOWLEDGEMENT

The authors wish to thank Mr. J. W. Lund for helpful discussions and suggestions, and Mr. J. Michaud for carrying out the programming and numerical computations.

27932

ABSTRACT

This report presents the analyses of longitudinal resonant modes of typical transducer configurations applicable to squeeze-film bearings. The transducer consists of a driving section and a driven extension on which the squeeze-film bearing is mounted. The extended section of the transducer is designed to provide amplification of excursions of the driving section. Three preliminary design configurations are proposed in this report as shown schematically in Figures 1, 2 and 3. Both a general analysis and a simplified approach are presented; design data are provided for each design configuration.

1. INTRODUCTION

In a squeeze-film bearing, the transducer converts the electrical input into a mechanical motion. In order to obtain the largest possible motion with a minimum power consumption, the transducer should be operated at resonance. While large motion of the transducer is desirable to achieve large load capacity of the squeeze-film bearing (refs. 1, 4 and 5), suspension of the transducer from its housing becomes a real problem. If rigid mounting of the transducer is to be made, the point of attachment to the transducer must be a node of its resonant mode. This requirement causes a bit of difficulty in the transducer-bearing configuration design. One satisfactory concept, which provides both radial and axial support of a float, is shown in Fig. 12. In this arrangement, the transducer would be operated at its longitudinal mode. Since the mid-plane is a natural node, it is a convenient location for the mounting flange. Conical (or spherical) bearing can support load in either direction even though the longitudinal transducer only provides axial squeeze-motion. However, the effective squeeze motion is reduced because only the component of the motion perpendicular to the bearing surface affects the gap. Thus it is even more important that the squeeze motion at the bearing be as large as possible.

Feasibility of achieving increased squeeze motion by elastically coupling the bearing element to the driven section of the transducer will be the main purpose of this study.

An analysis is presented for the lowest normal mode of longitudinal axial-excision transducers applicable to squeeze-film bearings. Three preliminary design configurations, shown schematically in Figs. 1, 2 and 3, are considered. It can be seen from those figures that each design consists of a driving section and a driven extension on which the squeeze-film bearing is mounted. The extended section of the transducer is designed to provide amplification of excursions of the driving section.

In Section 2, a thorough analysis is presented for each design configuration. Results are obtained in a form that allows numerical computations to be carried out easily. Section 3 offers a simplified analysis which brings out the major

controlling parameters and their effects. The relationships of the natural frequency of the system and of the amplitude of excursions of the squeeze-film bearing, as a function of the controlling parameters, are explicitly obtained. These relations are then presented in the form of design charts. A design procedure is suggested and examples are given at the end of Section 4.

2. GENERAL ANALYSIS

The configurations of the axial-excursion transducer are schematically illustrated in Figures 1, 2 and 3. These will be designated as configurations "A", "B" and "C", respectively.

2.1 Configuration "A"

In Configuration "A" (Figure 1) the center section of the transducer, made of piezoelectric ceramic core and metallic shells, is the driver. The piezoelectric core and the metallic shells are bonded together. In order to avoid thermal stresses at elevated temperatures, a specific metal was chosen that has a thermal coefficient of expansion matching that of the piezoelectric. Typical examples are molybdenum or Invar (42% Ni and 58% Fe) to match PZT-4 (Ref. 1). We choose the x^* -coordinate to be the distance from the central plane. We also assume a one-dimensional model for analysis — " x^* " is the only space coordinate required to describe the system. Thus, the configuration "A" may be visualized as its mechanical equivalent shown in Figure 1a. Note that the end flexure, having a mass much smaller than that of the bearing, is considered as a spring with spring constant k .

The equation of motion of longitudinal vibrations of an elastic rod is well-known (see e.g., Ref. 2). This will be applied to the composite circular cylinders in the central driving section ($0 < x^* < \alpha l$).

$$A_c E_c \frac{\partial^2 u^*}{\partial x^{*2}} + A_m E_m \frac{\partial^2 u^*}{\partial x^{*2}} = (\rho_c A_c + \rho_m A_m) \frac{\partial^2 u^*}{\partial t^{*2}} \quad (1)$$

where u^* is the local displacement, and A , E and ρ , respectively, denote area, Young's modulus and density. The symbols m and c indicate metal and ceramic respectively. It is to be emphasized here that A_m is the total cross-sectional area of the metallic shells. Equation (1) can be reduced to

$$\frac{E_1}{\rho_1} \frac{\partial^2 u^*}{\partial x^{*2}} = \frac{\partial^2 u^*}{\partial t^{*2}} \quad 0 < x^* < \alpha l \quad (2)$$

if we define

$$\begin{aligned}\rho_1 &= (\rho_c A_c + \rho_m A_m) / A_1 \\ E_1 &= (E_c A_c + E_m A_m) / A_1 \\ A_1 &= A_c + A_m\end{aligned}\quad (3)$$

Similarly we obtain

$$\frac{E_2}{\rho_2} \frac{\partial^2 v^*}{\partial x^{*2}} = \frac{\partial^2 v^*}{\partial t^{*2}} \quad \alpha l < x^* < l \quad (4)$$

where v^* is the displacement and $E_2 = E_m$, $\rho_2 = \rho_m$. And we have the following boundary conditions,

$$\begin{aligned}\text{The central plane is fixed in space:} \quad & u^* \Big|_{x^*=l} = 0 \\ \text{Compatibility:} \quad & u^* \Big|_{x^*=\alpha l} = v^* \Big|_{x^*=\alpha l} \\ \text{Force balance:} \quad & A_1 E_1 \frac{\partial u^*}{\partial x^*} \Big|_{x^*=\alpha l} = A_2 E_2 \frac{\partial v^*}{\partial x^*} \Big|_{x^*=\alpha l} \\ \text{Force balance:} \quad & -A_2 E_2 \frac{\partial v^*}{\partial x^*} \Big|_{x^*=l} - k(v^* \Big|_{x^*=l} - w^*) = \frac{m_s}{2} \frac{\partial^2 v^*}{\partial t^{*2}} \Big|_{x^*=l}\end{aligned}\quad (5)$$

The equation of motion of the bearing can be written as

$$-k(w^* - v^* \Big|_{x^*=l}) = (m_b + \frac{m_s}{2}) \frac{\partial^2 w^*}{\partial t^{*2}} \quad (6)$$

Here we have assumed that the end flexure is equivalent to a spring with spring constant k , and its mass, m_s , is lumped into two points, i.e., $\frac{m_s}{2}$ is attached to the bearing, and the other half is attached to location $x^*=l$. Justification of the validity of this assumption as well as a formula for k may be found in Appendix I.

If we define the following dimensionless variables,

$$\left. \begin{aligned} x &= \frac{x^*}{l} \\ t &= \omega t^* \\ u &= \frac{u^*}{l} \\ v &= \frac{v^*}{l} \\ w &= \frac{w^*}{l} \end{aligned} \right\} \quad (7)$$

then, the above equations become

$$\frac{E_1}{\omega^2 l^2 \rho_1} \frac{\partial^2 u}{\partial x^2} = \ddot{u} \quad 0 < x < \alpha \quad (8)$$

$$\frac{E_2}{\omega^2 l^2 \rho_2} \frac{\partial^2 v}{\partial x^2} = \ddot{v} \quad \alpha < x < 1 \quad (9)$$

$$u(0, t) = 0 \quad (10)$$

$$u(\alpha, t) = v(\alpha, t) \quad (11)$$

$$\frac{\partial u(\alpha, t)}{\partial x} = \frac{A_2 E_2}{A_1 E_1} \frac{\partial v(\alpha, t)}{\partial x} \quad (12)$$

$$- \frac{A_2 E_2}{l} \frac{\partial v(1, t)}{\partial x} - k [v(1, t) - w] = \frac{m_s}{2} \omega^2 \frac{\partial^2 v(1, t)}{\partial t^2} \quad (13)$$

$$- k [w - v(1, t)] = (m_b + \frac{m_s}{2}) \omega^2 \frac{\partial^2 w}{\partial t^2} \quad (14)$$

To obtain the solutions of Eqs. (8) and (9), we assume that

$$u(x, t) = U(x) \exp(it) \quad (15)$$

$$v(x, t) = V(x) \exp(it) \quad (16)$$

Then, by using Eq. 10, it is a simple matter to obtain

$$U(x) = C_1 \sin(\omega l \sqrt{\frac{\rho_1}{E_1}} x) = C_1 \sin(\frac{\pi}{2} \frac{\omega}{\omega_1} x) \quad (17)$$

$$\text{and } V(x) = C_2 \sin \left[\omega \ell \sqrt{\frac{\rho_2}{E_2}} (x - x_0) \right] = C_2 \sin \left[\frac{\pi}{2} \frac{\omega}{\omega_2} (x - x_0) \right] \quad (18)$$

$$\text{where } \omega_1 = \frac{\pi}{2\ell} \sqrt{\frac{E_1}{\rho_1}} \quad (19)$$

$$\omega_2 = \frac{\pi}{2\ell} \sqrt{\frac{E_2}{\rho_2}}$$

C_1 and C_2 are amplitudes of excursions; ω_1 and ω_2 are characteristic frequencies of the respective section; and x_0 is a phase angle to be determined from the boundary conditions.

Using Eqs. (11) through (14), we get

$$\frac{C_2}{C_1} = \frac{\sin\left(\frac{\pi}{2} \alpha \frac{\omega}{\omega_1}\right)}{\sin\left[\frac{\pi}{2} \frac{\omega}{\omega_2} (\alpha - x_0)\right]} \quad (20)$$

$$\beta = \frac{1 + \gamma}{\frac{E_c}{E_m} + \gamma} \frac{\omega_1}{\omega_2} \tan\left(\frac{\pi}{2} \alpha \frac{\omega}{\omega_1}\right) \cot\left[\frac{\pi}{2} \frac{\omega}{\omega_2} (\alpha - x_0)\right] \quad (21)$$

$$\frac{C_3}{C_2} = \frac{A_2 E_2}{\ell k} \frac{\pi}{2} \frac{\omega}{\omega_2} \cos\left[\frac{\pi}{2} \frac{\omega}{\omega_2} (1 - x_0)\right] + \left[1 - \left(\frac{\omega}{\omega_s}\right)^2\right] \sin\left[\frac{\pi}{2} \frac{\omega}{\omega_2} (1 - x_0)\right] \quad (22)$$

$$\text{and } \frac{C_3}{C_2} \left[1 - \left(\frac{\omega}{\omega_b}\right)^2\right] = \sin\left[\frac{\pi}{2} \frac{\omega}{\omega_2} (1 - x_0)\right] \quad (23)$$

$$\text{where } \omega_s = \sqrt{\frac{k}{m_s/2}}$$

$$\omega_b = \sqrt{\frac{k}{m_b + \frac{m_s}{2}}} \quad (24)$$

$$\beta = A_1/A_2$$

$$\gamma = A_m/A_c$$

and C_3 is the amplitude of excursions of the bearing, i.e.,

$$w = C_3 \exp(it) \quad (25)$$

From Eqs. (20) through (23) we have four equations with four unknowns (providing that the dimensions and the material constants are all given): C_2/C_1 , ω , x_0 and C_3/C_1 . Due to the form of Eqs. (20) through (23), it is convenient to start the calculation from a given value of ω . Consequently, one of the input data, preferably A_1 or m_b , must be kept floating. The procedure for numerical calculation is as follows:

Input Data

l , α , γ , materials constants, A_2 , m_b and dimensions of the flexure. Note that A_1 is not given.

- a) Assume a value of ω .
- b) Calculate E_1 , ρ_1 , ω_1 , ω_2 , ω_s , ω_b and k .
- c) Eliminate C_3/C_2 from Eqs. (22) and (23) to obtain

$$\frac{A_2 E_2}{l k} \frac{\pi}{2} \frac{\omega}{\omega_2} \operatorname{ctn} \left[\frac{\pi}{2} \frac{\omega}{\omega_2} (1-x_0) \right] + \left[1 - \left(\frac{\omega}{\omega_s} \right)^2 \right] = \left[1 - \left(\frac{\omega}{\omega_b} \right)^2 \right]^{-1} \quad (26)$$

From Eq. (26), the value of x_0 may be solved numerically.

- d) Calculate C_2/C_1 and $\beta (= A_1/A_2)$ from Eqs. (20) and (21) respectively. Here, A_1 has been chosen to replace ω as an unknown quantity as indicated before.
- e) Calculate the amplitude amplification factor from

$$\frac{C_3}{C_1 \sin \left(\frac{\pi}{2} \frac{\omega}{\omega_1} \alpha \right)} = \left[1 - \left(\frac{\omega}{\omega_b} \right)^2 \right]^{-1} \cdot \frac{\sin \left[\frac{\pi}{2} \frac{\omega}{\omega_2} (1-x_0) \right]}{\sin \left[\frac{\pi}{2} \frac{\omega}{\omega_2} (\alpha-x_0) \right]} \quad (27)$$

Note that β may turn out to be an exceedingly large number or even a negative number. The latter is physically unrealistic as β , defined as the area ratio, A_1/A_2 , must be positive. It is then necessary to assume a new value of k or m_b until a reasonable and desired combination of β and $C_3 / \left[C_1 \sin \left(\frac{\pi}{2} \frac{\omega}{\omega_1} \alpha \right) \right]$ is reached. If several sets of values of β

and amplitude amplification are obtained, the criterion should be that the strain level at the central plane be as small as possible. The strain can be expressed as

$$\epsilon = \frac{\partial u^*}{\partial x^*} = C_1 \frac{\pi \omega}{2 \omega_1} \cos\left(\frac{\pi \omega}{2 \omega_1} x\right) e^{i\omega t^*} \quad (28)$$

$$\text{and } \epsilon_o = \left. \frac{\partial u^*}{\partial x^*} \right|_{x^*=t^*=0} = C_1 \frac{\pi \omega}{2 \omega_1} \quad (28a)$$

Hence, we add

f) Calculate and maximize

$$\frac{C_3}{\epsilon_o} = \left(\frac{\pi \omega}{2 \omega_1}\right)^{-1} \left[1 - \left(\frac{\omega}{\omega_b}\right)^2\right]^{-1} \sin\left(\frac{\pi \omega}{2 \omega_1} \alpha\right) \frac{\sin\left[\frac{\pi \omega}{2 \omega_2} (1-x_o)\right]}{\sin\left[\frac{\pi \omega}{2 \omega_2} (\alpha-x_o)\right]} \quad (29)$$

2.2 Configuration "B"

In Configuration "B" (Figure 2), there is no end flexure as compared to Configuration "A" (Figure 1). The area of the extended section, A_2 , is reduced by cutting slots and/or reducing the thickness of the shells. The reduction of A_2 will obviously decrease the rigidity of the extended section; this, in turn, is expected to result in amplification in the excursions of the bearing.

It is not difficult to see that the analysis for Configuration "A" is applicable to this case, except that the boundary conditions at $x = 1$ (Eq. (13) and Eq. (14) are replaced by

$$-\frac{A_2 E_2}{l} \frac{\partial v(1,t)}{\partial x} = m_b \omega^2 \frac{\partial^2 v(1,t)}{\partial t^2} \quad (30)$$

which may readily be simplified to

$$\tan\left[\frac{\pi \omega}{2 \omega_2} (1-x_o)\right] = \frac{\pi A_2 E_2}{2 m_b \omega \omega_2 l} \quad (30a)$$

Then the procedure for numerical computation is as follows:

Input Data: ℓ , α , γ , material constants, A_2 and m_b .

- a) Assume a value of ω .
- b) Solve Eq. (30a) for x_o .
- c) Compute β from Eq. (21).
- d) Calculate the amplitude ratio

$$\frac{|v(\ell, t)|}{|u(\alpha\ell, t)|} = \frac{C_2 \left[\sin \frac{\pi}{2} \frac{\omega}{\omega_2} (1-x_o) \right]}{C_1 \sin \left(\frac{\pi}{2} v \right)} = \frac{\sin \left[\frac{\pi}{2} \frac{\omega}{\omega_2} (1-x_o) \right]}{\sin \left[\frac{\pi}{2} \frac{\omega}{\omega_2} (\alpha-x_o) \right]} \quad (31)$$

$$\text{and } \frac{|v(\ell, t)|}{\alpha \epsilon_o} = \frac{\sin \left[\frac{\pi}{2} \frac{\omega}{\omega_2} (1-x_o) \right]}{\sin \left[\frac{\pi}{2} \frac{\omega}{\omega_2} (\alpha-x_o) \right]} \cdot \frac{\sin \left(\frac{\pi}{2} v \right)}{\frac{\pi}{2} v}$$

$$\text{where } v = \alpha \frac{\omega}{\omega_1}$$

- e) Adjust m_b until a reasonable and desired combination of β and amplitude ratio is obtained.

It is noted that in order to achieve a high amplitude ratio, x_o should be close to α . Then, the last factor in Eq. (21), $\cot \left[\frac{\pi}{2} \frac{\omega}{\omega_2} (\alpha-x_o) \right]$, and consequently β becomes very large. This indicates that heavy driving section is required.

For $\alpha = 1$, there is the special case that amplification of the transducer motion is due to mass loading effect alone. This will be further discussed in Section 3.2.

2.3 Configuration "C"

In Fig. 3, Configuration "C" is shown to have the same basic features as the Configuration "A", although there is only one metallic shell sandwiched by two piezoelectric shells. The end flexures are again provided to amplify the excursion amplitude of the squeeze-film bearing. The analysis for Configuration "A" still applies here if the symbols are properly identified; e.g., A_c and A_m represent respectively the cross-sectional area of the ceramic and the metal in the driving

section. Their values should be calculated from the geometry of the corresponding design configuration. Note that k should be computed by Eq. (I-8) instead of (I-7) — Appendix I.

3. SIMPLIFIED ANALYSIS

In this chapter a simplified analysis is performed on the results derived in Section 2.

3.1 Configurations "A" and "C"

Since one of the major purposes of the transducer is to provide a relatively high amplitude amplification, $\frac{C_3}{C_1 \sin(\frac{\pi}{2} \frac{\omega}{\omega_1} \alpha)}$, it is seen from Eq. (27) that ω_b must be close to ω . Also, Eq. (24) indicates that

$$\omega_s \gg \omega_b \approx \omega \quad (33)$$

since m_b is much larger than m_s . Eq. (26) is then reduced to

$$\frac{A_2 E_2}{\ell k} \frac{\pi \omega}{2 \omega_2} \operatorname{ctn} \left[\frac{\pi \omega}{2 \omega_2} (1-x_o) \right] = -1 + \left[1 - \left(\frac{\omega}{\omega_b} \right)^2 \right]^{-1}$$

or

$$\frac{A_2 E_2}{\ell k (1-x_o)} \approx -1 + \left[1 - \left(\frac{\omega}{\omega_b} \right)^2 \right]^{-1} \quad (34)$$

where $x_o \approx 1$ and we have used the approximation

$$\operatorname{ctn} \left[\frac{\pi \omega}{2 \omega_2} (1-x_o) \right] = \left[\frac{\pi \omega}{2 \omega_2} (1-x_o) \right]^{-1} \quad (35)$$

We may further assume that $\alpha \lesssim 1$, i.e., we do not need a "long" extended section which merely serves as a connection between the driving section and the end flexure. Thus,

$$x_o \approx \alpha \approx 1 \quad (36)$$

and Eq. (21) can be written as

$$\frac{A_1 E_1}{A_2 E_2} = \frac{\omega_1}{\omega_2} \left[\frac{\pi \omega}{2 \omega_2} (\alpha - x_o) \right]^{-1} \tan \left(\frac{\pi}{2} v \right) \quad (37)$$

where $v = \alpha \frac{\omega}{\omega_1}$

Combining Eqs. (34) and (37), we obtain

$$\frac{\pi}{2} \left(\frac{A_1 E_1}{\ell k} \right) \left(\frac{\omega_b}{\omega_1} \right) \operatorname{ctn} \left(\frac{\pi}{2} v \right) = \frac{\omega/\omega_b}{1 - (\omega/\omega_b)^2} \quad (38)$$

Also, Eqs. (27) and (29) may be approximated as

$$\frac{C_3}{C_1 \sin(\frac{\pi}{2} v)} = \left[1 - \left(\frac{\omega}{\omega_b} \right)^2 \right]^{-1} \quad (39)$$

and

$$\frac{C_3}{\alpha \epsilon_o} = \left(\frac{\pi}{2} v \right)^{-1} \sin(\frac{\pi}{2} v) \left[1 - \left(\frac{\omega}{\omega_b} \right)^2 \right]^{-1} \quad (40)$$

Rearrangement of Eqs. (38), (39) and (40) yields, respectively

$$\frac{A_1 E_1}{k \alpha \ell} = \frac{(A_1 \rho_1 \alpha \ell / m_b)}{(\frac{\pi}{2} v)^2} - \frac{\tan(\frac{\pi}{2} v)}{\frac{\pi}{2} v} \quad (38a)$$

$$\frac{C_3}{C_1 \sin(\frac{\pi}{2} v)} = \frac{\operatorname{ctn}(\frac{\pi}{2} v)}{\frac{\pi}{2} v} \left(\frac{A_1 \rho_1 \alpha \ell}{m_b} \right) \quad (39a)$$

and

$$\frac{C_3}{\alpha \epsilon_o} = \frac{\cos(\frac{\pi}{2} v)}{(\frac{\pi}{2} v)^2} \left(\frac{A_1 \rho_1 \alpha \ell}{m_b} \right) \quad (40a)$$

Eqs. (38a), (39a) and (40a) are plotted in the form of design charts (Section 4).

3.2 Configuration "B"

For the general case that $\alpha < 1$, it is recommended that one use the procedures suggested in Section 2.2. In this section we shall present the special case of $\alpha = 1$, i.e., there is no extended section; the squeeze-film bearing is directly mounted at the end of the driver.

The boundary condition at $x^* = l$ is

$$-\frac{A_1 E_1}{l} \frac{\partial u(1,t)}{\partial x} = m_b \omega^2 \frac{\partial^2 u(1,t)}{\partial t^2} \quad (41)$$

On using Eq. (17), we obtain

$$\frac{\pi}{2} \frac{A_1 E_1}{m_b l \omega \omega_1} = \tan \left(\frac{\pi}{2} \frac{\omega}{\omega_1} \right) \quad (42)$$

Thus, by rearranging terms, we have for $\alpha = 1$ the simple equation

$$\frac{A_1 \rho_1 l}{m_b} = \frac{\pi}{2} \frac{\omega}{\omega_1} \tan \left(\frac{\pi}{2} \frac{\omega}{\omega_1} \right) \quad (42a)$$

and

$$\begin{aligned} \frac{C_3}{\epsilon_0} &= \frac{u(1,t)}{\frac{\partial u}{\partial x}(0,t)} \\ &= \frac{\sin\left(\frac{\pi}{2} \frac{\omega}{\omega_1}\right)}{\left(\frac{\pi}{2} \frac{\omega}{\omega_1}\right)} \end{aligned} \quad (43)$$

4. DESIGN DATA, PROCEDURES AND ILLUSTRATIVE EXAMPLES

The design charts for Configurations "A" and "C", generated from Equations (38a), (39a) and (40a) are presented in Figures 4, 5 and 6. Figures 4 and 5 are cross-plotted to give Fig. 7 which shows lines of constant $\frac{C_3}{\alpha \epsilon_0}$. Figure 6 is a plot of amplitude amplification versus dimensionless mass ratio with v as parameter. In the next section we shall illustrate the design procedure by an example.

Design Procedure for Configurations "A" and "C"

Example

Input Data

$$A_1 = 2 \text{ in}^2$$

$$l = 3/4 \text{ in}$$

$$\gamma = 0.1$$

Use molybdenum and PZT-4.

$$E_m = 47 \times 10^6 \text{ psi}$$

$$\rho_m = 0.355 \text{ lb/cu.in}$$

$$E_c = 12.9 \times 10^6 \text{ psi}$$

$$\rho_c = 0.271 \text{ lb/cu.in}$$

$$\text{a. Compute } E_1 = \frac{E_c + \gamma E_m}{1 + \gamma} = 16 \times 10^6 \text{ psi}$$

$$\rho_1 = \frac{\rho_c + \gamma \rho_m}{1 + \gamma} = 0.278 \text{ lb/cu.in}$$

$$\begin{aligned} \omega_1 &= \frac{\pi}{2l} \sqrt{\frac{E_1}{\rho_1}} = \frac{\pi}{2 \times 0.75/12} \sqrt{\frac{16 \times 10^6 \times 144}{0.278 \times 12^3 / 32.2}} \\ &= 3.12 \times 10^5 \text{ rad/sec} \end{aligned}$$

$$\text{b. Assume } \alpha = 0.94$$

$$\text{and } \omega = 1.33 \times 10^5 \text{ rad/sec.}$$

$$\text{Then } v = \alpha \frac{\omega}{\omega_1} = 0.4$$

c. Assume $k = 1.28 \times 10^8$ lb/ft

$$\text{Then } \frac{A_1 E_1}{k \alpha l} = 4.25$$

d. Read from Figure 4

$$\frac{A_1 \rho_1 \alpha l}{m_b} = 2.13$$

$$\underline{m_b = 5.7 \times 10^{-3} \text{ slug}}$$

e. Read from Figure 7

$$\frac{C_3}{C_1 \sin(\frac{\pi}{2} v)} = 4.6$$

f. Read from Figure 5

$$\frac{C_3}{\alpha \epsilon_o} = 4.4$$

The value of $k = 1.28 \times 10^8$ lb/ft in (d) is not difficult to achieve inasmuch as the spring constant k given by Eq. (I.7) or (I.8) for Configuration "A" or "C" can yield a wide range of values by various designs. From (b), (e) and (f), $\omega = 1.33 \times 10^5$ rad/sec = 21.2 k.c./sec, $\frac{C_3}{C_1 \sin(\frac{\pi}{2} v)} = 4.6$ and $\frac{C_3}{\alpha \epsilon_o} = 4.4$, these

values are likely to satisfy the need of a squeeze-film bearing. If, however, these values together with the bearing mass ($m_b = 5.7 \times 10^{-3}$ slug = 0.183 lb.) are not satisfactory. One should then start a new calculation by assuming, e.g., a new value of v or $\frac{A_1 E_1}{k \alpha l}$.

The above calculations yield all the design information except the value of A_2 . The area A_2 as seen in Figure 1 or 3 is the total cross-sectional area of the short stubs. Physically, A_2 is not a dominant factor for the transducer because the short stubs serve only as a connection to link the driving section and the flexure and the squeeze-film bearing. Thus, it is not surprising that A_2

in the simplified analysis, no longer appears. The value of A_2 can only be obtained from the general analysis.

We continue the above example by following the procedure suggested in Section 2.1 in the general analysis. By so doing we obtain

- a. A_2
- b. A check of accuracy of the simplified analysis.

Input Data

$$\alpha = 0.94$$

$$l = 3/4 \text{ in}$$

$$\gamma = 0.1$$

Use molybdenum and PZT-4.

- a. Compute $E_1 = 16 \times 10^6 \text{ psi}$
 $\rho_1 = 0.278 \text{ lb/cu.in}$
 $\omega_1 = 3.12 \times 10^5 \text{ rad/sec}$

- b. Assume $\omega = 1.33 \times 10^5 \text{ rad/sec}$
 Thus $v = \alpha \frac{\omega}{\omega_1} = 0.4$

- c. Assume for the time being a value of $A_2 = 0.25 \text{ in}^2$ instead of a value of A_1 . We shall later compute A_1 from Eq. (21).

- d. From $k = 1.28 \times 10^8 \text{ lb/ft}$, we can design the flexure as:

Configuration "A"

$$N = 32 = \text{number of beams in each metallic shell.}$$

$$D = 2\frac{1}{2} \text{ in}$$

$$b = 0.0625 \text{ in}$$

$$h = 0.0374 \text{ in}$$

which results in

$$\begin{aligned}
 k &= 2 \frac{192 E_2 b h^3 N^4}{12(\pi D)^3} \\
 &= 1.067 \times 10^7 \text{ lb/in} \\
 &= 1.28 \times 10^8 \text{ lb/ft}
 \end{aligned}
 \tag{I-7}$$

e. Assume $m_b = 5.7 \times 10^{-3}$ slug

From Eq. (26) we find

$$x_o = 0.554$$

f. Compute β from Eq. (21)

$$\beta = \frac{A_1}{A_2} = 11.73$$

$$A_1 = 0.25 \times 11.73 = 2.93 \text{ in}^2$$

g. Compute

$$\frac{C_3}{C_1 \sin(\frac{\pi}{2} \nu)} = 6.8$$

h. Run the calculation for different values of m_b from 4.5×10^{-3} to 6.5×10^{-3} slug.

i. Repeat the above calculations for $A_2 = 0.125 \text{ in}^2$ which is one-half of the previous assumed value.

The results are plotted in Figures 8 and 9. It is seen from Figure 8 ($A_2 = 0.25$) that for $A_1 = 2 \text{ in}^2$, m_b should be 5.3×10^{-3} slug, and the amplitude amplification is approximately 5.0. From Figure 9 ($A_2 = 0.125 \text{ in}^2$) for $A_1 = 2 \text{ in}^2$, m_b should be 5.13×10^{-3} slug and the amplitude amplification is again approximately 5.0.

The above results indicate that:

- a. A_2 is indeed unimportant.
- b. The simplified analysis yields an m_b whose value is about 10 percent higher than that of the general analysis.

However, if one insists on $m_b = 5.7 \times 10^{-3}$ slug and chooses $A_2 = 0.25 \text{ in}^2$, then the natural frequency, ω , of the system will be changed. The graphs in Figure 10 show that, at $A_1 = 2 \text{ in}^2$, $\omega = 1.28 \times 10^5 \text{ rad/sec}$, and the amplitude amplification is 4.8. The natural frequency is only about 4 percent off the value $1.33 \times 10^5 \text{ rad/sec}$; and the amplitude amplification is about 4.5 percent off the value 4.6. Hence, we conclude that the simplified analysis is a good approximation.

Design Procedure for Configuration "B"

It is seen from Eq. (32) that in order to have a relatively high amplitude amplification, α should not be close to unity.

Example

Input Data

$$\begin{aligned}\alpha &= 0.6 \\ l &= 3/4 \text{ in} \\ \gamma &= 0.1 \\ A_2 &= 0.25 \text{ in}^2 \\ m_b &= 6.0 \times 10^{-3} \text{ slug} \\ \text{Use molybdenum and PZT-4.} \\ E_2 = E_m &= 47 \times 10^6 \text{ psi}\end{aligned}$$

$$\begin{aligned}\text{a. Calculate } E_1 &= 16 \times 10^6 \text{ psi} \\ \rho_1 &= 0.278 \text{ lb/cu.in} \\ \omega_1 &= 3.12 \times 10^5 \text{ rad/sec.}\end{aligned}$$

$$\text{b. Assume } \omega = 2.07 \times 10^5 \text{ rad/sec} = 33 \text{ k.c./sec}$$

$$\text{Thus } v = \frac{\omega}{\omega_1} \alpha = 0.4$$

c. From Eq. (30a) we find

$$x_o = 0.276$$

d. From Eq. (21) we calculate

$$\beta = \frac{A_1}{A_2} = 7.41$$

$$A_1 = 1.85 \text{ in}^2$$

e. From Eqs. (31) and (32), we obtain

$$\frac{v(l,t)}{u(\alpha l,t)} = 2.45$$

$$\text{and } \frac{v(l,t)}{\alpha \epsilon_o} = 2.2 \quad \therefore \frac{v(l,t)}{\epsilon_o} = 1.33$$

f. Repeat the above calculations for different values of m_b . The results are plotted in Figure 11. It is then seen that for $A_1 = 2 \text{ in}^2$

$$\frac{v(l,t)}{u(\alpha l,t)} = 2.6$$

$$\text{and } \frac{v(l,t)}{\alpha \epsilon_o} = 2.35 \quad \therefore \frac{v(l,t)}{\epsilon_o} = 1.41$$

From the above examples we make the following comparison:

Configuration	$A_1(\text{in})$	α	$\omega(\text{k.c./sec})$	$m_b(\text{slug})$	$u(1,t)$	$\frac{C_3}{C_1 \sin(\frac{\pi}{2}v)}$	$\frac{C_3}{\epsilon_o}$	v
"A" or "C"	2	0.94	21.2	5.7×10^{-3}	$C_1 \sin(\frac{\pi}{2}v)$	4.6	4.14	0.4
"B"	2	0.60	33	6.2×10^{-3}	$C_1 \sin(\frac{\pi}{2}v)$	2.6	1.41	0.4

It is seen from the above table that for the same size driver and the same displacement at $x = \alpha$, Configuration "A" provides larger excursion amplitude for the squeeze-film bearing than Configuration "B".

5. CONCLUSIONS

The axial-excursion transducer of a squeeze-film bearing was studied analytically. Both a general analysis and a simplified analysis are presented. The results of the simplified analysis for Configurations "A" and "C" have been plotted in the form of design charts. An example is given in Section 4, which illustrates the procedures for using the design charts. The same problem was reworked by using the general analysis and the results were found to be very close to those obtained from the design charts. For Configuration "B", a design procedure is suggested in Section 2.2. It was found that, in general, Configurations "A" and "C" with a properly designed end flexure do provide larger amplitude amplifications than Configuration "B"; also, for each corresponding design configuration larger amplitude amplification can be achieved by increasing the size of the driving section.

Thus, increased excursion amplitude can be obtained at the expense of increase configuration complexity. In the ascending order of achievable excursion amplitude, the rankings of the considered configurations are:

1. Configuration "B" without the extended section ($\alpha = 1$).
2. Configuration "B" with an extended section ($\alpha < 1$).
3. Configuration "A"
4. Configuration "C".

Further increase of the excursion amplitude can only be achieved by providing a larger driving section for Configuration "A" or "C".

REFERENCES

1. Pan, C.H.T., Editor, "Analysis, Design and Prototype Development of Squeeze-Film Bearings for AB-5 Gyro," MII Report 64TR66, 1964.
2. Flugge, W., Editor, "Handbook of Engineering Mechanics," McGraw-Hill, 1962, pp. 61-62.
3. Roark, R.J., "Formulas for Stress and Strain," McGraw-Hill, 1954.
4. Salbu, E.O.J., "Compressible Squeeze-Films and Squeeze Bearings", Trans. ASME, Journal of Basic Engineering, Vol. 86, Series D, No. 2, June 1964.
5. Malanoski, S.B., and Pan, C.H.T., Discussion of Ref. 4, loc. cit., pp. 364-366.

APPENDIX I - FLEXURE CALCULATION

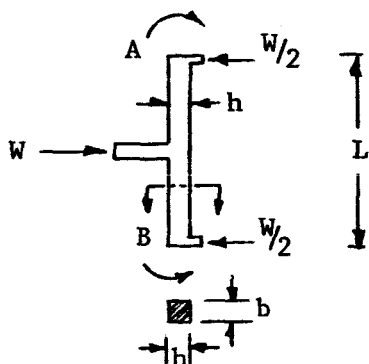


Figure I-1.

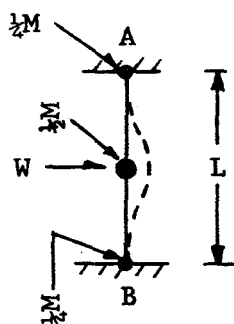


Figure I-2.

Each unit cell of the flexure in Fig. 1 may be visualized as a beam structure. Because of symmetry, the deflection curve at the supporting points (A and B in Fig. I-1) has a zero slope. Consequently the beam may be considered to have both ends built in as shown in Fig. I-2 (left). When the beam is vibrating, a typical deflection curve at a particular instant would appear as indicated by the dotted line in Fig. I-2. Were we to lump half of the beam mass ($M/2$) at the center and to attach $M/4$ to each end point A and B, we would obtain an approximate formula for the natural frequency of the beam

$$\omega_{\text{beam}} = \sqrt{\frac{W/\delta}{\frac{1}{2}M}} \quad (\text{I-1})$$

where δ = deflection at the center of the beam.

From Reference 3, we have

$$\delta = \frac{WL^3}{192 EI} \quad (\text{I-2})$$

Substitution of Eq. (I-2) into Eq. (I-1) results in

$$\omega_{\text{beam}} = 19.6 \sqrt{\frac{EI}{ML^3}} \quad (\text{I-3})$$

An exact formula in Reference 2 (p. 61-69) shows that the frequency of the lowest mode is

$$\omega_{\text{beam}}^{(1)} = (4.73^2) \sqrt{\frac{EI}{ML^3}} = 22.4 \sqrt{\frac{EI}{ML^3}} \quad (\text{I-4})$$

Although the discrepancy between the approximate and the exact formulae is about 12 percent, the result will be greatly improved if we bring the mass of the squeeze-film bearing into the picture. The bearing mass is estimated roughly at 10 times heavier than that of the sum of the masses of all the beams.

We will now obtain a spring constant, k , for the flexure which is by definition

$$k = \frac{P}{\delta} \quad (I-5)$$

where P is the total force acting on the flexure and

$$\begin{aligned} P &= 2 NW \quad \text{for Configuration "A"} \\ &= NW \quad \text{for Configuration "C"} \end{aligned} \quad (I-6)$$

N denotes the number of beams in each shell and the factor of 2 in the first part of Eq. (I-6) represents that there are two metallic shells in Configuration "A".

Combining Eqs. (I-2), (I-5) and (I-6) and using the relationships $L = \frac{\pi D}{N}$ and $I = \frac{1}{12} bh^3$, we obtain

$$k = \begin{cases} 2 \frac{192 E_2 N^4 bh^3/12}{(\pi D)^3} & \text{for Configuration "A"} \\ \frac{192 E_2 N^4 bh^3/12}{(\pi D)^3} & \text{for Configuration "C"} \end{cases} \quad (I-7)$$

$$(I-8)$$

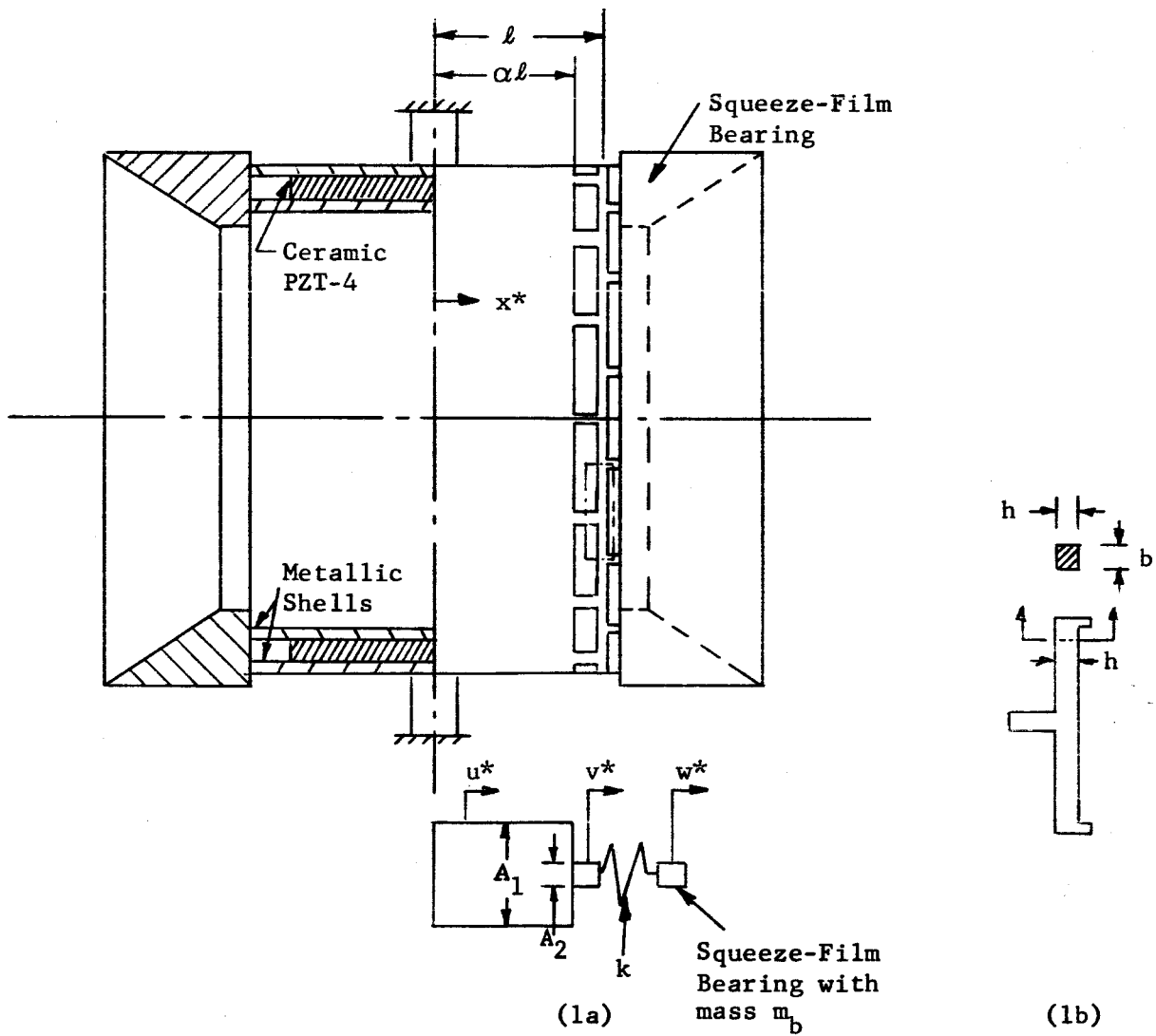


Fig. 1 Transducer Configuration "A"

- (a) Sketch of the Mechanical Equivalent of Configuration "A"
- (b) Enlarged View

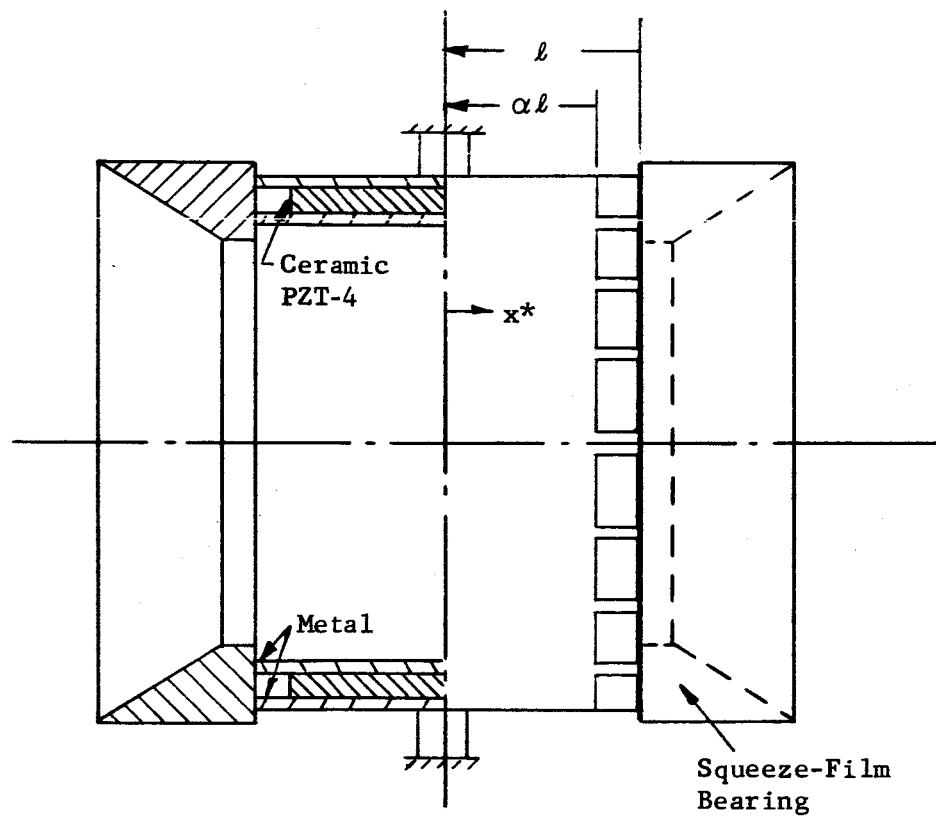


Fig. 2 Transducer Configuration "B"

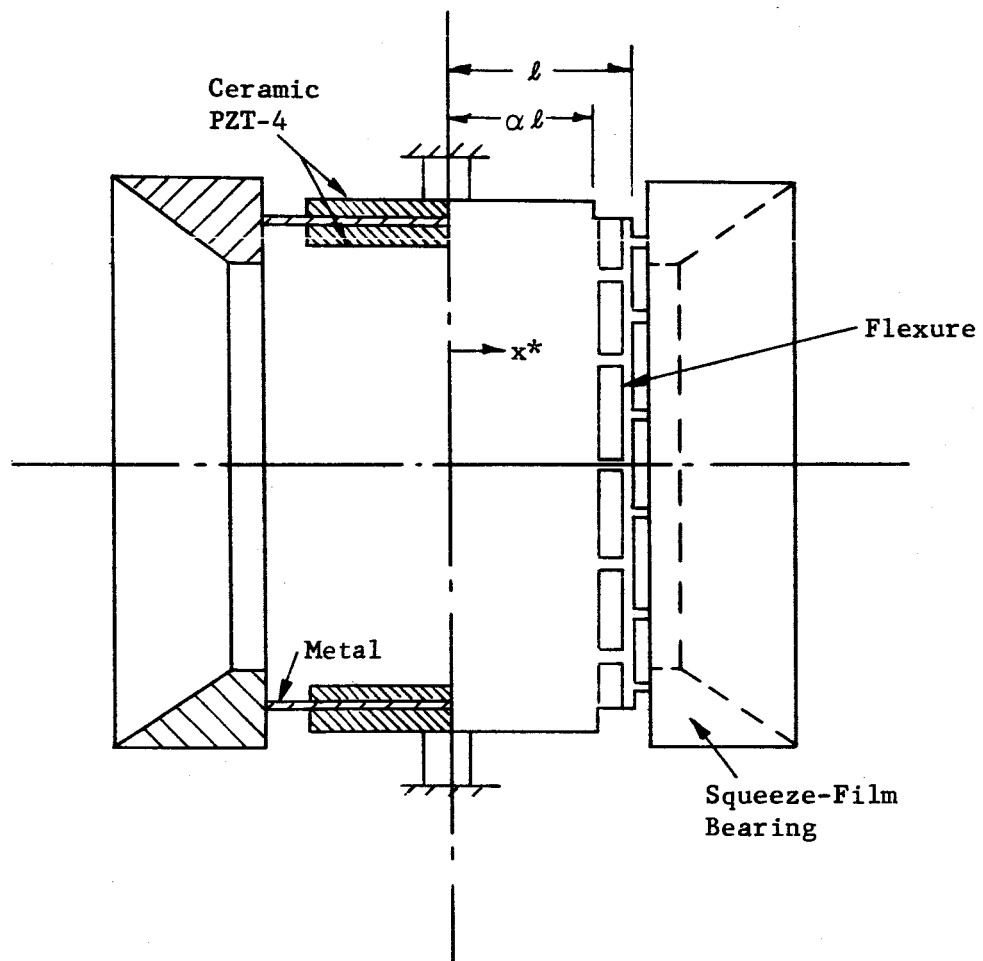


Fig. 3 Transducer Configuration "C"

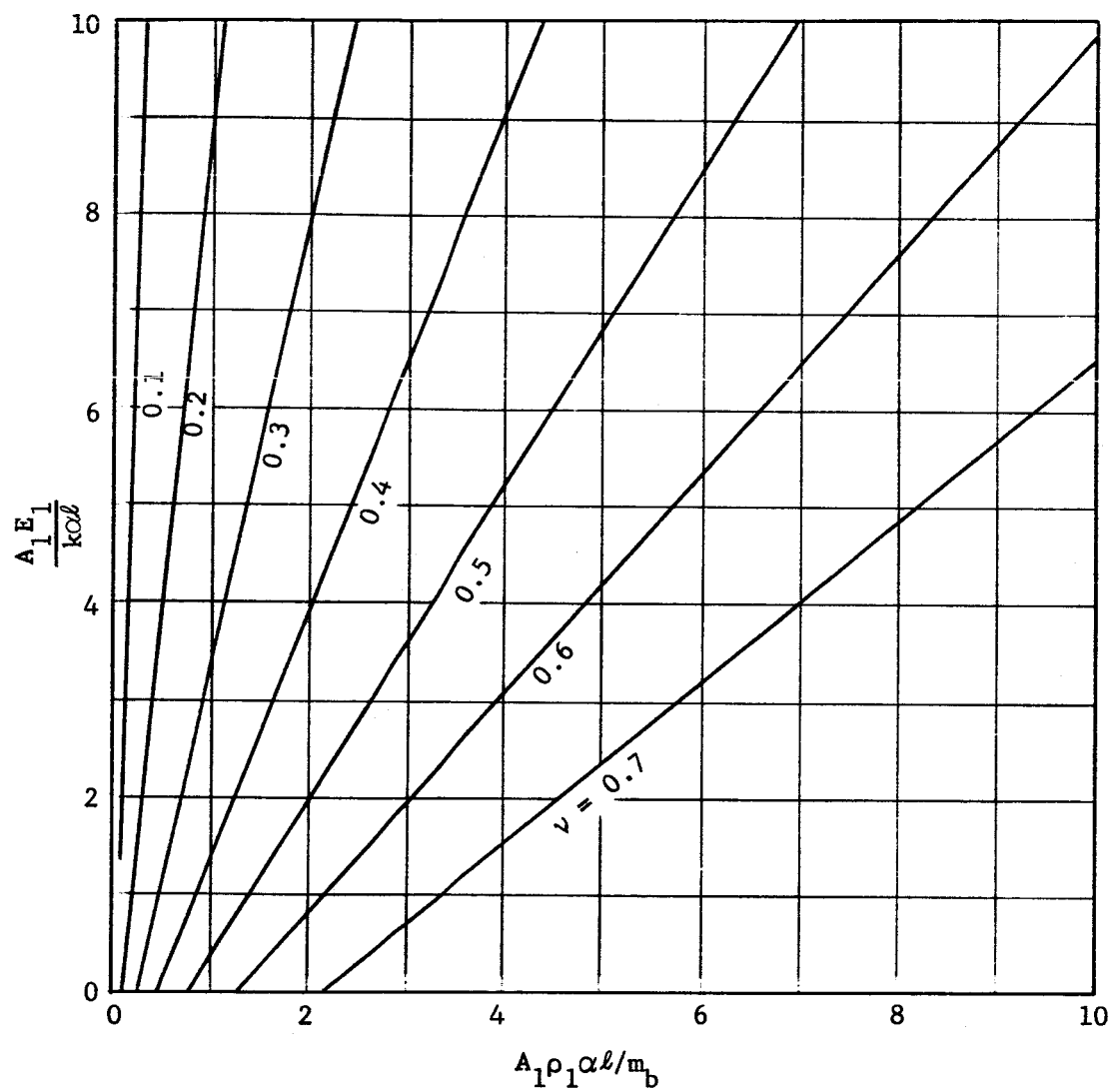


Fig. 4 $\frac{A_1 E_1}{k \alpha l}$ against $\frac{A_1 \rho_1 \alpha l}{m_b}$; Configuration "A"

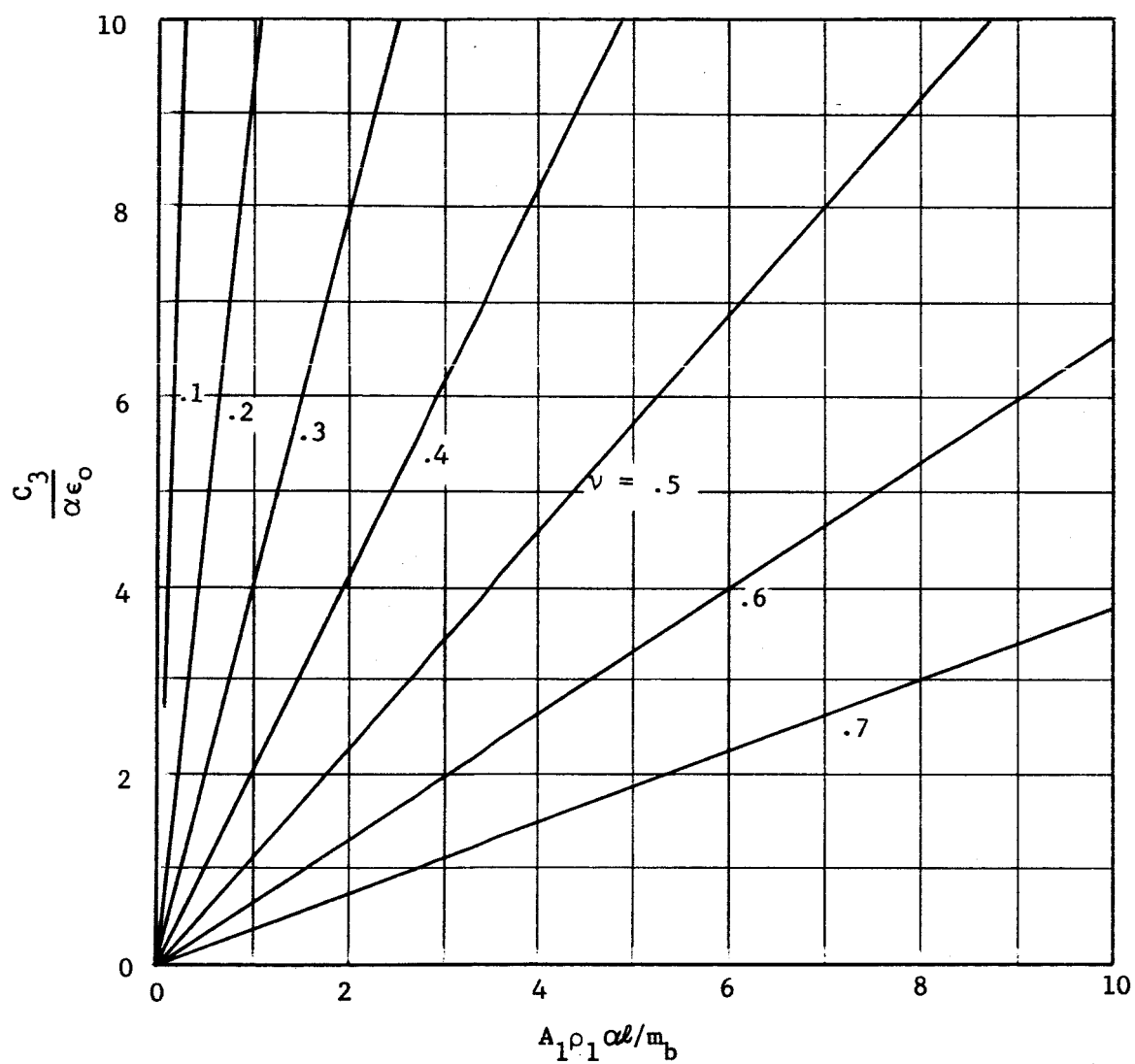


Fig. 5 $\frac{C_3}{\alpha \epsilon_0}$ against $\frac{A_1 \rho_1 \alpha l}{m_b}$; Configuration "A"

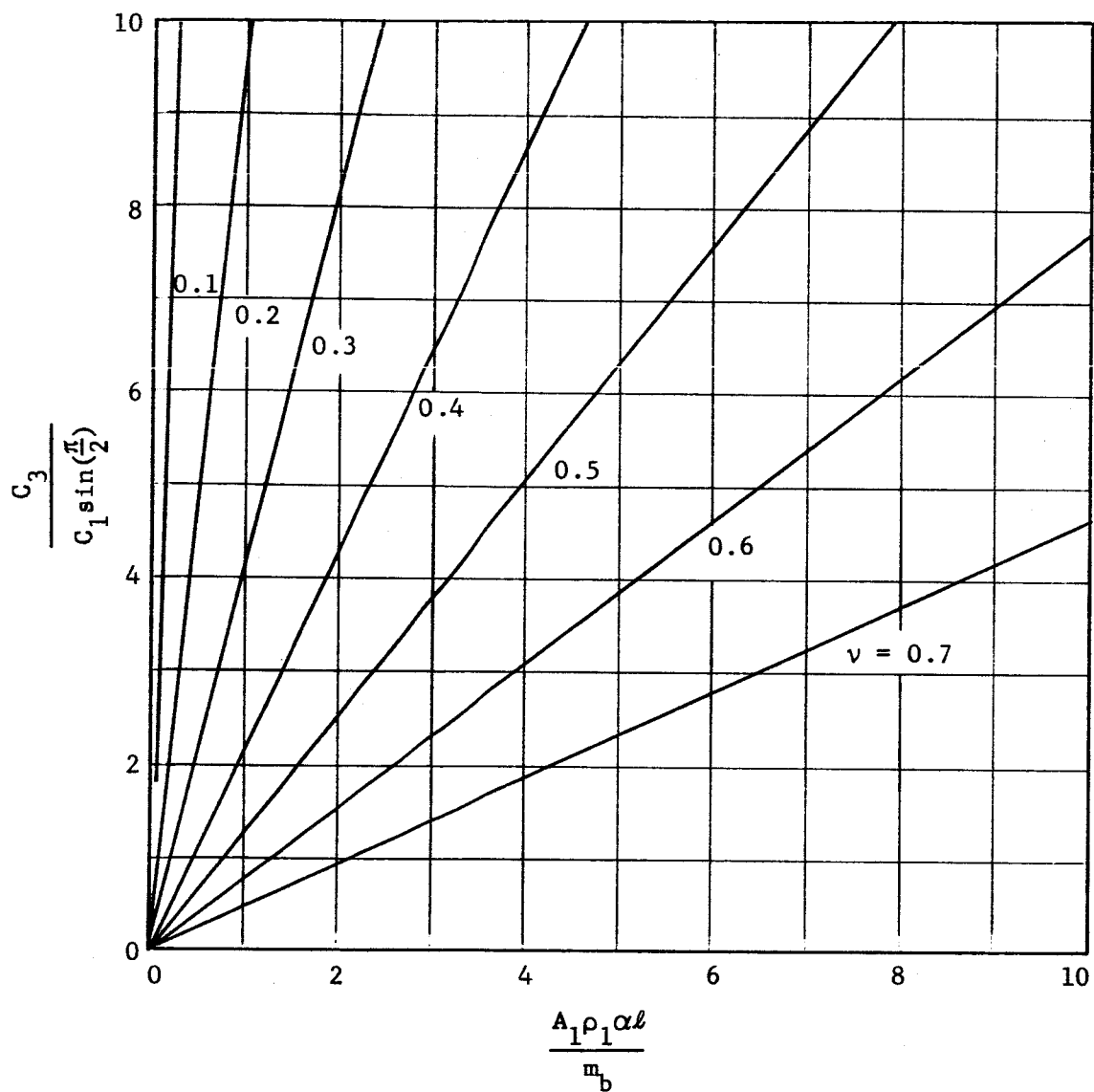


Fig. 6 Amplitude Amplification versus Dimensionless Mass Ratio; Configuration "A"

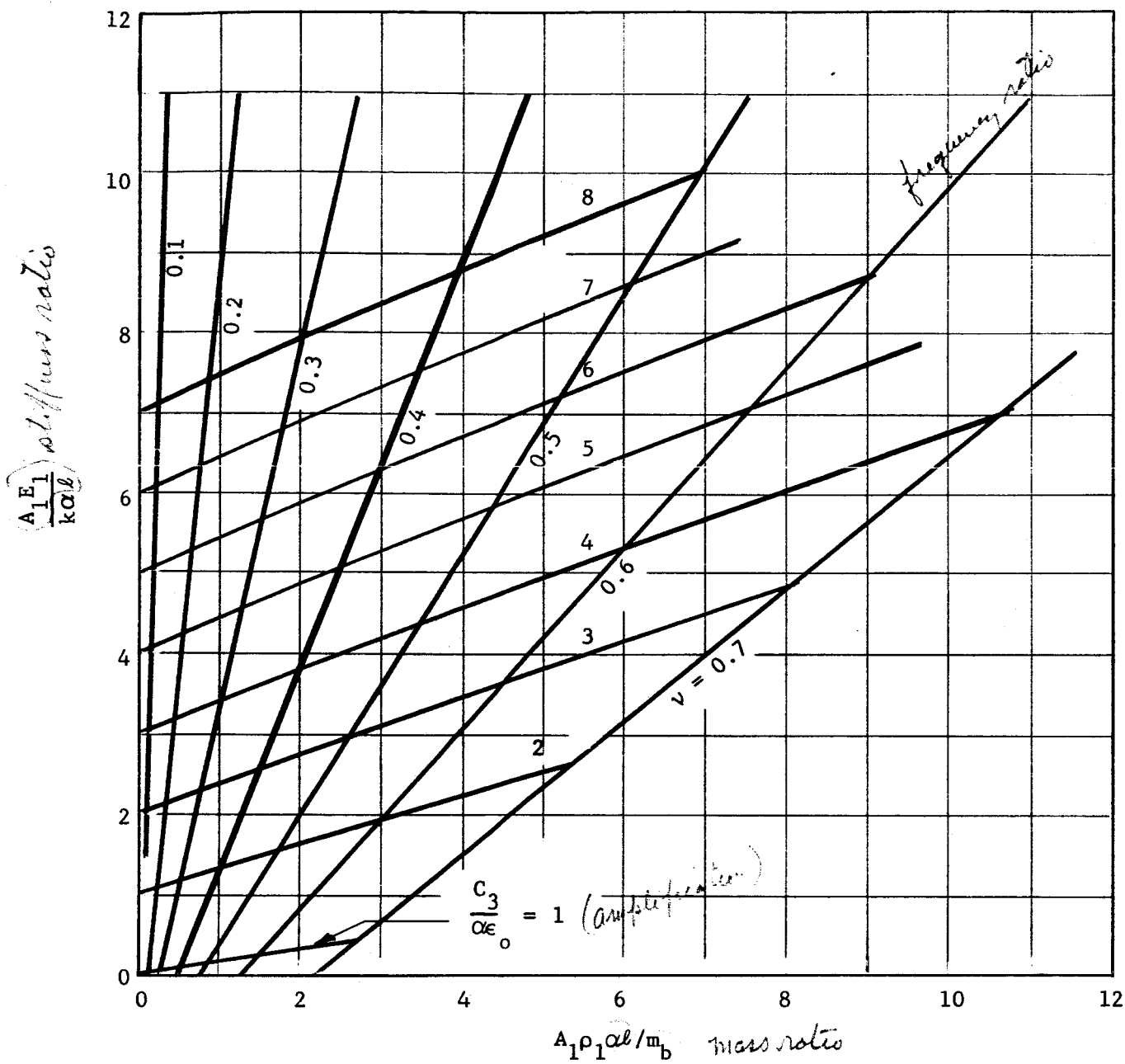


Fig. 7 $\frac{A_1 E_1}{k \alpha l}$ against $\frac{A_1 \rho_1 \alpha l}{m_b}$ with Lines of Constant ν and

Lines of Constant $\frac{C_3}{\alpha \epsilon_0}$; Configuration "A"

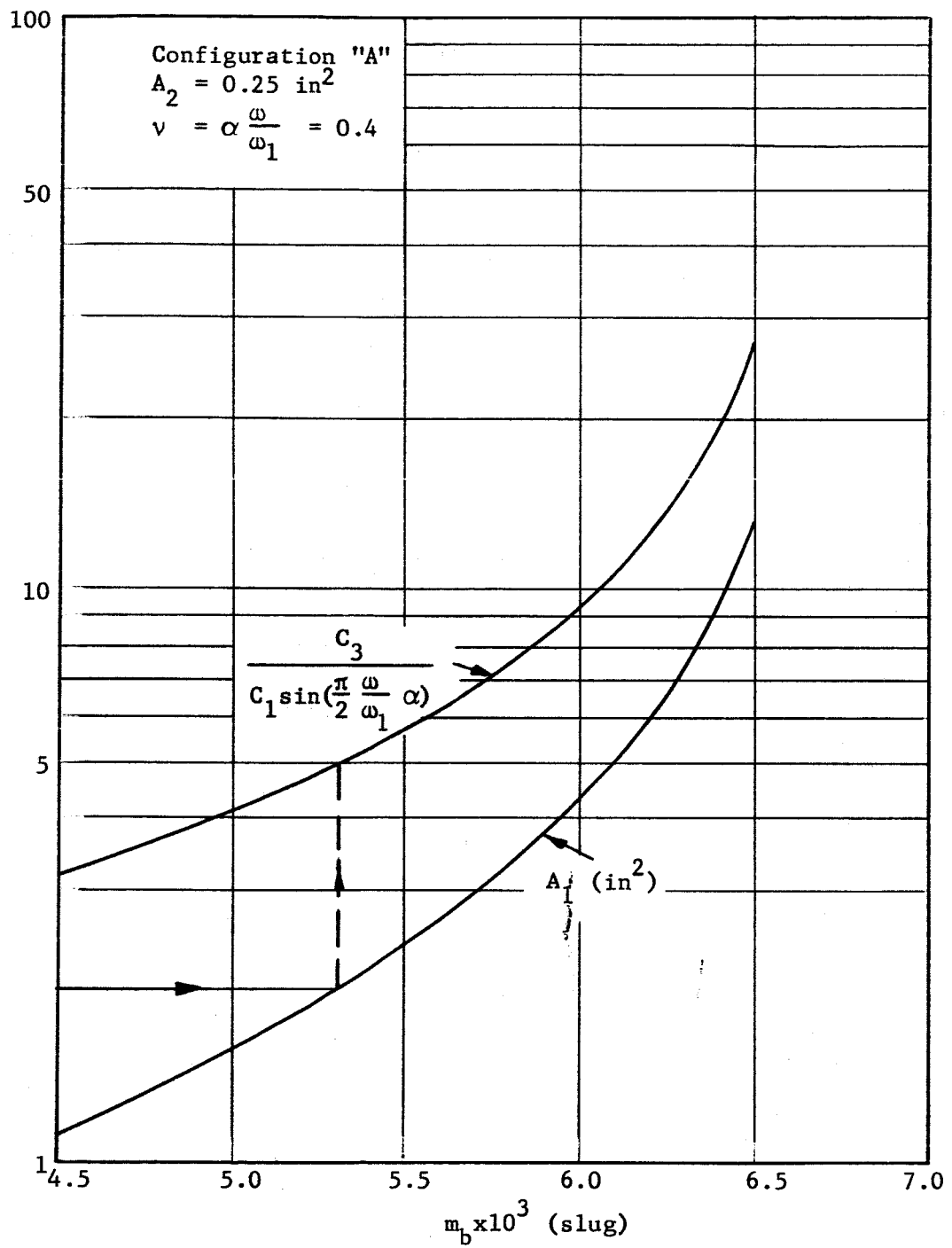


Fig. 8 A_1 and Amplitude Ratio versus m_b for $A_2 = 0.25 \text{ in}^2$

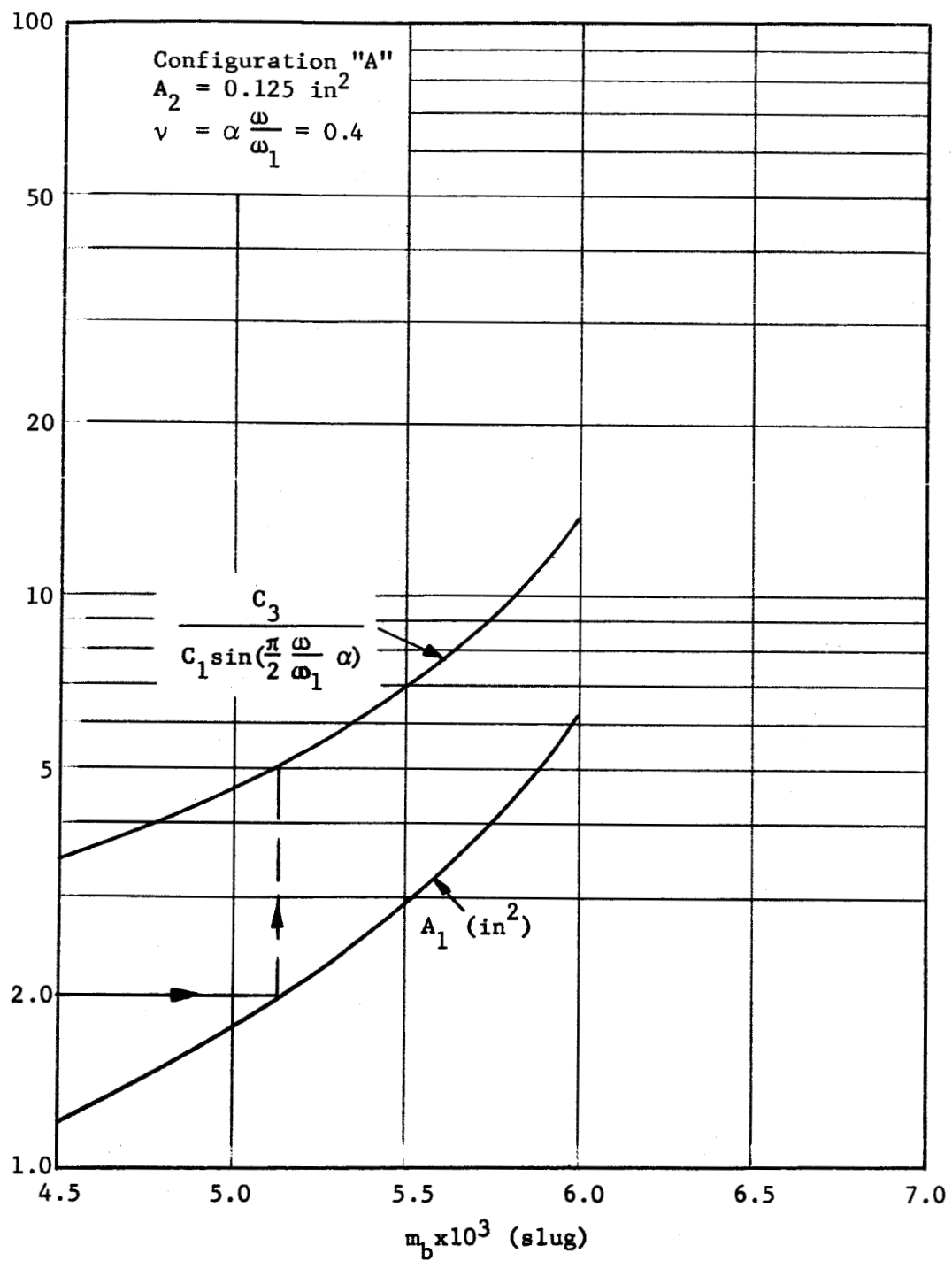


Fig. 9 A_1 and Amplitude Ratio versus m_b for $A_2 = 0.125 \text{ in}^2$

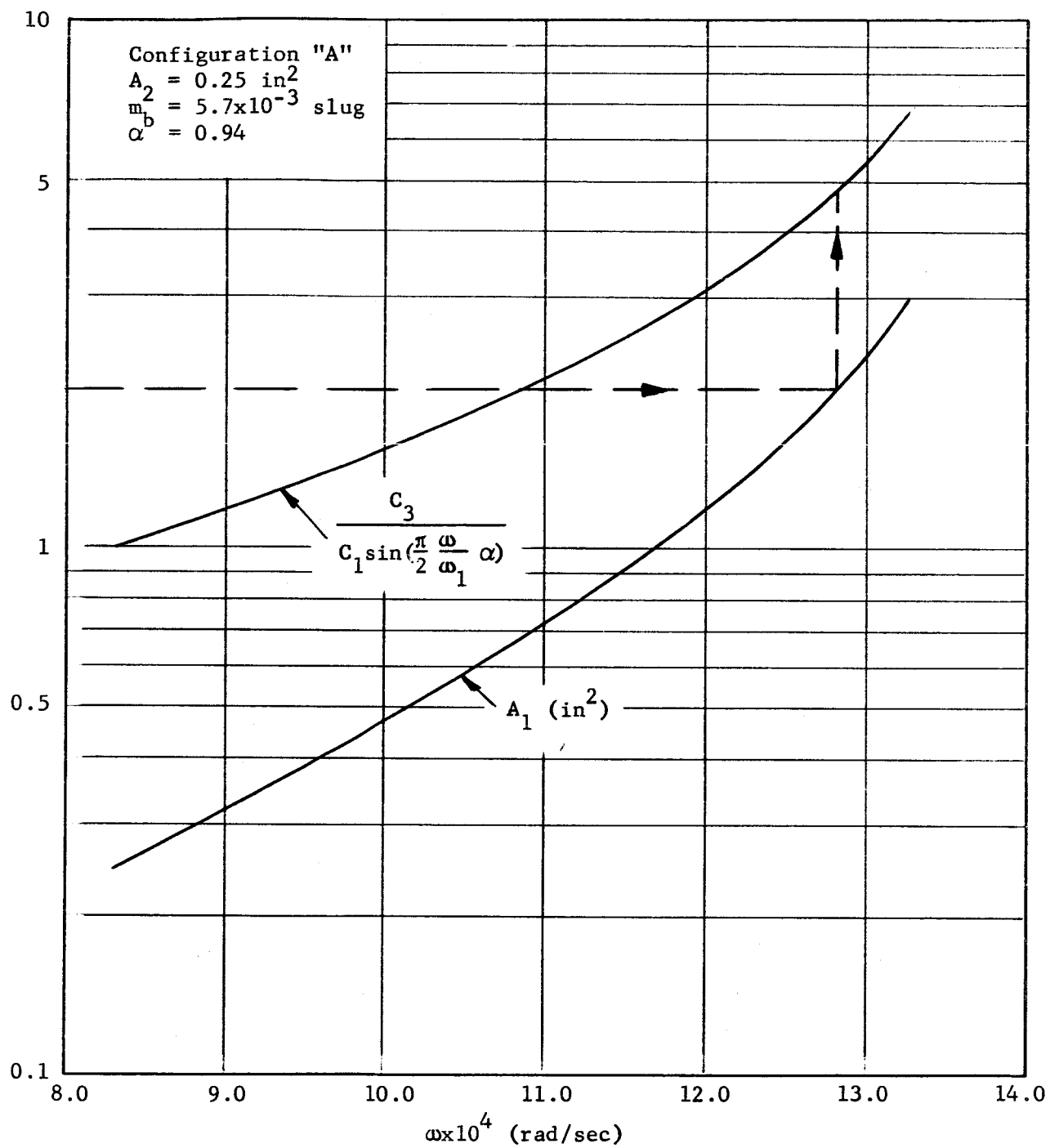


Fig. 10 A_1 and Amplitude Ratio versus ω for Configuration "A"

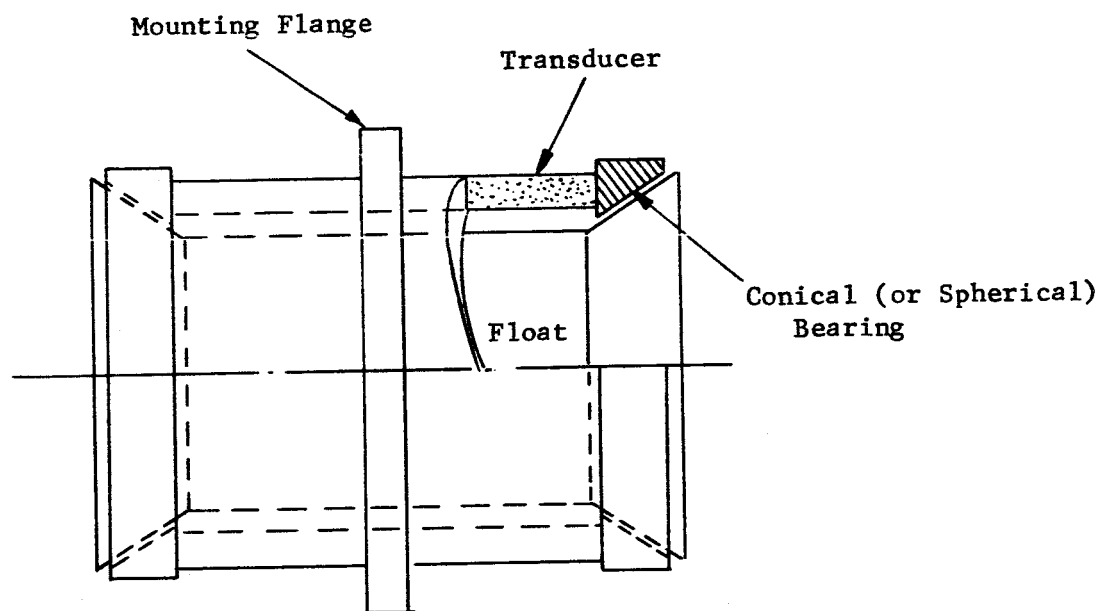


Fig. 12 Combined Radial and Axial Squeeze-Film Bearing
Driven by Longitudinal Transducer

NOMENCLATURE

A	area
b	width of the beam cross-section
C_1, C_2, C_3	defined in Eqs. (17), (18) and (25)
D	diameter
E	Young's modulus
h	height of the beam cross-section
I	moment of inertia
k	equivalent spring constant
l	length of the transducer from the central plane (Fig. 1)
m	mass
N	number of beams per cylindrical shell
P	total force on end flexure
t^*	time
t	ωt^* , dimensionless time
u, v, w	dimensionless displacements
U, V	amplitudes of displacements
x	dimensionless coordinate
x_0	a phase angle defined in Eq. (18)
α	ratio of the length of the driving section to the total length (Fig. 1)
β	A_1/A_2
γ	A_m/A_c
δ	deflection
ν	$\alpha \frac{\omega}{\omega_1}$
ρ	density
ω	frequency

Subscripts

c	ceramic
m	metal
s	spring
b	bearing
1	driving section, $0 < x < \alpha$
2	extended section, $\alpha < x < 1$
3	bearing

Superscripts

*	dimensional quantities
---	------------------------